IEEE Access
Multidisciplinary | Rapid Review | Open Access Journal

Received June 5, 2021, accepted June 15, 2021, date of publication June 23, 2021, date of current version July 1, 2021.

Digital Object Identifier 10.1109/ACCESS.2021.3091293

Islanding Detection for Inverter-Based Distributed Generation Using Unsupervised Anomaly Detection

ADEEL ARIF[1], (Member, IEEE), KASHIF IMRAN[1], QIUSHI CUI[2], (Member, IEEE), AND YANG WENG[2], (Senior Member, IEEE)

[1]U.S.-Pakistan Center for Advanced Studies in Energy (USPCAS-E), National University of Sciences and Technology (NUST), Islamabad 44000, Pakistan
[2]School of Electrical and Computer Engineering, Arizona State University, Tempe, AZ 85281, USA

Corresponding author: Kashif Imran (kashifimran@uspcase.nust.edu.pk)

This work was supported by USAID through the prestigious research exchange program at Arizona State University.

ABSTRACT Islanding detection with the rising grid supporting inverter-based distributed generation is becoming more critical protection due to its high droop gains and overall decreased system inertia leading to rapid changes in the electrical parameters. Traditional methods for islanding detection in this regard are susceptible to significant problems such as non-detection zone, false-positive detection, and inefficient mode of validation. Therefore, to attenuate these problems, this paper proposes a hybrid islanding detection technique based on unsupervised anomaly detection using autoencoders. This technique uses the rate of change of frequency as primary and phase angles of the voltage and current as secondary detection parameters, demonstrating improved performance, reliability, and robustness due to its shared advantage of both active frequency drift and autoencoder. Furthermore, a dialectic model of offline and online validation schemes is also proposed to ensure the reliability of detection. Extensive simulations and validations have been carried out on multiple networks to generate data sets used to train, test, and validate the technique and compute its statistical significance, thereby confirming its effectiveness. The optimal islanding detection time for the base cases was recorded as 20 milliseconds with an F1-score of 0.991, dependability index of 0.998, security index of 0.995, with total harmonic distortion of 4.56% and zero non-detection zones, which complies with IEC 61000-3-2 and IEEE standard 1547's requirement of detection within two seconds after islanding.

INDEX TERMS Islanding, distributed power generation, microgrids, unsupervised learning.

I. INTRODUCTION

'Renewables-2020', a report published by International Energy Agency (IEA) forecasts a thirty-three percent share of renewables in total electricity generation by 2025. This corresponds to the fact that 2,257 TWh of additional renewable electricity generation is about to be added within a period of five years, which is twenty-three percent of the current renewable generation capacity of the world [1]. This will create a huge demand for sophisticated control, optimization, and management technologies to address the challenges and risks associated with this expansion. With this rising distributed energy resources (DER) penetration in the existing system, islanding detection (or loss of main) will be critical protection to ensure equipment and personal safety and avoid false tripping leading to cascaded outages. Islanding detection has been a classical problem whose literature is widely scattered over the technical comparisons of its non-detection zone (NDZ), methodology of implementation, inverter configuration type, System type, selectivity of tripping criteria, and fault ride-through cases.

A. THE ISLANDING DETECTION PROBLEM

According to IEEE, ''islanding is defined as a condition in which a portion of the utility system that contains both load and distributed resources remains energized while isolated from the remainder of the utility system'' [2]. Thus, DERs isolated under such conditions are called islanded and the portion of the system including the islanded DER along with the local load is regarded as an island. It is analogous to consider a grid supporting inverter-based DER as a current source that is connected to the local load and the grid. During islanding,

The associate editor coordinating the review of this manuscript and approving it for publication was Shafi K. Khadem.

especially for a shorter duration, the loss of grid reference parameters for the inverter may introduce a large phase error difference eventually resulting in an asynchronous re-closure with large surge currents damaging the DER itself [3]. On the other hand, the presence of voltage on the grid side can be hazardous for the maintenance team. Therefore, it is standardized by IEEE std. 1547.2018, to detected islanding within two seconds after the occurrence of the event [4], [5].

B. CLASSIFICATION OF ISLANDING EVENTS

Islanding events have been categorized into various types based on their duration, nature of causality, topology, and operational philosophy. For instance, islanding events with a run on times of less than a second are classified as 'short termed' whereas islanding events with a run on times equal to one second or more are classified as 'long termed' [3]. Islanding events have also been categorized into 'intentional' or 'unintentional', with intentional islanding events, further sub-categorized into scheduled and unscheduled [4]. Scheduled intentional islanding is usually performed by means of a local operator at the DER or through a manual operation by grid operator or maybe through an advance control operation such as an Automatic Generator Control (AGC). Unscheduled intentional islanding is an autonomous operation that occurs as a result of an anomaly at the node of interconnection between DER and the grid.

The topological classification for islanding events is split into 'remote' and 'local' methods, such that, remote methods are traditionally telecommunication based and are relatively expensive to deploy than a local method. These methods include transfer trips [6] and power line carrier [7]. Local methods are more popular and are known for their superior accuracy, selectivity, and reliability. These are sub-categorized into 'active' and 'passive' methods. Active methods are characterized by techniques that usually introduce a small perturbation into the inverter current as an active feature for islanding detection, whereas passive methods do not change the characteristics of the system at all and purely rely on the sensor-based approaches, which may include analog or data-driven techniques. Active and passive methods are further discussed critically in the next section.

Over time, passive methods have been greatly improved using data-driven techniques. Nevertheless,U. Markovic, *et al.* in [8] have presented a satisfactory argument for the ineffectiveness of passive islanding detection methods with the increasing grid supporting DERs. However, the initiatives to improve active methods using data-driven techniques are rarely seen in the literature. This is due to their complicated methodology of implementation in the inverter control and their already superior selectivity to the NDZ problem compared to traditional passive methods.

This inspired us to propose a hybrid islanding detection technique based on the combination of active frequency drift and unsupervised learning, which does not only demonstrates a shared advantage of active early detection and intelligent leaning based methodology at the same time but also advocates its statistical significance by an F1-score of 0.991, dependability index of 0.998 and security index of 0.995. It was observed from the past unsupervised learning-based approaches that a single training parameter such as voltage (sag/swell) can lead to nuisance tripping due to its sensitivity towards the load variations and high impedance faults [9]. For this reason, we selected three out of six best parameters for our training, which were validated in a dialectical mode of operation, i.e. online and offline.

The major contribution of the proposed technique is to establish a framework for intelligent detection schemes based on adaptive/learnable settings (i.e. cost/error function) rather than programmed settings for physical parameters. This means that the pickup of the fault is not restricted to any specific threshold of electrical parameter, rather it is dependent on the dissimilarity index of the subjected signal with the trained signal. Secondly, the proposed technique also presents a framework capable of quantifying the statistical significance of intelligent islanding detection schemes based on the values of its indices and dialectic mode of validation. furthermore, the technique also promises to be computationally very efficient, fast responding, and low-quality compromising. This is due to the autoencoder, which is exceptionally efficient for anomaly detection applications, especially for complex non-linear pattern recognition problems using dimensionality reduction.

This article is arranged into sections as follows: Section II discusses the background of islanding detection methods. Section III discusses the technical implications of unsupervised anomaly detection for the islanding detection problem. The detailed hierarchical methodology for islanding detection is proposed in section IV. Section V demonstrates the base case simulation results and statistical significance of the technique. Then finally, the discussion and conclusive remarks are made n order to compare the effectiveness of the proposed technique in comparison with the other recently published techniques in section VI and section VII respectively.

II. ISLANDING DETECTION METHODS

IEEE 1547 demonstrates a standard model to explain and analyze the characteristics of an islanding condition, as shown in Fig. 1. In this model, node 'O' represents the common intersection between the load, the grid, and the DER. This common node of intersection is formally called point of common coupling (PCC). Before islanding, the power flow from DER to the PCC can be stated as $P_{DG} + jQ_{DG}$ and the power flowing from PCC to the local load can be stated as $P_{load} + jQ_{load}$. The utility grid in such a situation may be providing or consuming power which can be mathematically expressed as:

$$\Delta P = P_{load} - P_{DER} \tag{1}$$

$$\Delta Q = Q_{load} - Q_{DER} \tag{2}$$

During islanding conditions, ΔP and ΔQ converges to zero as neither power is absorbed nor supplied by the gird.

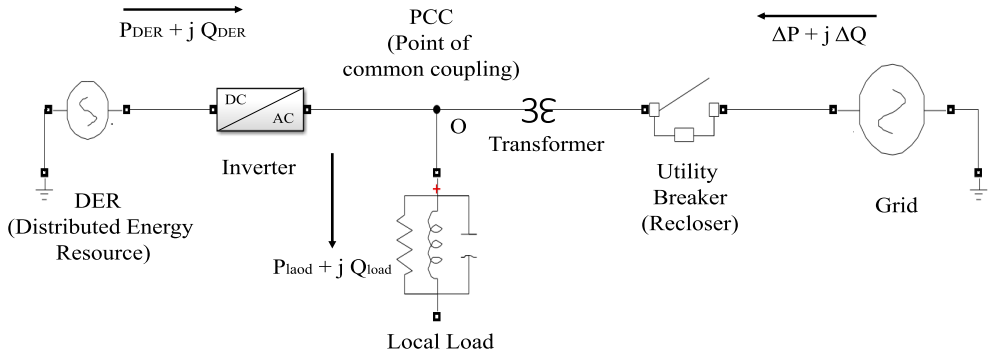

FIGURE 1. IEEE 1547 model for islanding detection.

However, the values of the voltage and frequency are determined by the residual conditions (1) (2), which may exceed the upper or lower limit of the over/under frequency relay (U/OFR) or over/under voltage relay (U/OVR) [3]. The operating parameter limits defined by IEEE Std 929 and IEEE 1547 are considered as a benchmark for simulation and experiments for islanding as shown in table 4. (see appendix)

Power mismatch case is usually referred to as the condition when $\Delta P = \Delta Q = 0$. It is the case when either the active power produced by DER has matched the load's consumption or the load-displacement power factor at resonant frequency has converged to unity (i.e. $\omega_o = \omega_{res}$). Under such circumstances, there are no significant changes in voltage and frequency during the islanding event and as a result, the U/OFR and U/OVR are unable to detect islanding, thus forming an NDZ.

The non-detection zone (NDZ) for an inverter-based islanding detection method (IDM) is determined by the selectivity of its non-detection over its active and reactive power mismatch conditions. It is a function of its inverter control topology which is classified broadly into two categories, i.e. grid forming and grid supporting inverter controls. Grid forming inverters are governed by droop control law and use self-computed values for subsequent voltage and frequency utilizing active and reactive power set-points. For this reason, they behave analogous to voltage sources in an electrical power system (EPS), with standalone characteristics of their own. Gird following inverters, on the other hand, are not standalone inverters and they totally rely on the on-grid system's voltage and frequency values to compute their active and reactive power response. Therefore, in this inverter control topology, the inverter behaves analogously to a current source. Grid following inverter control is considered as one of the significant and underdeveloped areas in modern power systems. These can be further divided into grid feeding (constant power) and grid supporting inverters (constant current). The grid feeding inverters are designed to give constant power output to the EPS (i.e. both gains are set to zero). However, the grid supporting inverters provide a dynamic power output based on their predefined gains to

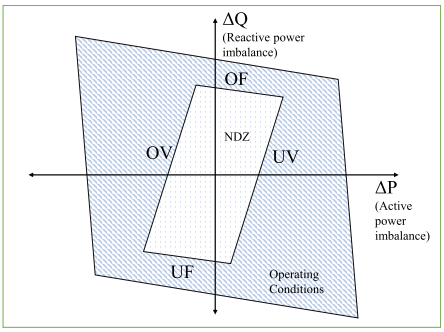

FIGURE 2. Non-detection zone for power mismatch cases.

support the grid in all conditions [8]. The NDZ characteristics of a grid feeding inverter can be described mathematically as (3) (4) and visualized as shown in Fig. 2.

$$\frac{V^2}{V^2_{max}} - 1 \leq \frac{\Delta P}{P_G} \leq \frac{V^2}{V^2_{min}} - 1 \tag{3}$$

$$Q_f \left(1 - \frac{f^2}{f^2_{min}}\right) \leq \frac{\Delta Q}{P_G} \leq Q_f \left(1 - \frac{f^2}{f^2_{max}}\right) \tag{4}$$

Passive methods usually detect islanding directly through traditional relaying (OV, UV, OF, UF) without changing the electrical characteristics of the power system. Few classical passive methods are based on the rate of change of frequency (ROCOF) [10], rate of change of voltage phase angle [11] and vector shift [12]. But these methods suffer from a large NDZ problem. Selecting a threshold for passive islanding trip settings is difficult to determine, and arbitrary low values can result in nuisance tripping. However, the NDZ problem can be improved by various techniques based on frequency domain and data-driven approaches [13]. Popular frequency-domain methods are based on discrete wavelet transforms [14], [15], harmonic distortions [16], mathematical morphology [17] and duffing oscillators [18]. Similarly data-driven methods are usually based on decision tree [19], random forest [20], support vector machine (SVM) [21], and neural network [9].

Active methods are based on perturbing and observing principles. These are slightly complex to implement and are based on distorting the inverter current wave by a frequency

drift operation as shown in Fig. 5. During islanding conditions the frequency drift augmented to the inverter current creates a large change in active and reactive power flow at the PCC, resulting in a drastic change in voltage and frequency (5) (6). This increases the chances of U/OVR and U/OFR tripping and detection of islanding earlier than the traditional methods. Traditional active methods include active frequency drift (AFD) [22], slip mode phase shift (SMS) [23], sandia frequency shift (SFS) [24] and positive feedback-based methods [25].

$$P_{load} = V_0 \frac{V_0}{R_{load}} \tag{5}$$

$$Q_{load} = V_0 \left[\frac{V_0}{\omega L} - \frac{V_0}{(1/\omega C)} \right] \tag{6}$$

The recently presented literature about classical active islanding includes positive feedback-based control loop designs. In [26], a linear feedback loop is designed to improve the NDZ problem with a total harmonic distortion (THD) ranging from 1.68-2.68% under different loading conditions. Moreover, a composite islanding technique was presented in [27], which uses voltage and frequency-based detection with an improvised definition of chopping factor based on harmonic injections. The technique claims to reduce the THD of the classical AFD by 60%. On the other hand, [28] and [29] presents d and q axis-based islanding detection schemes that utilize either pattern watchdog schemes or band-pass filters and mean of absolute frequency variation-based schemes.

The classical active techniques as stated above, in general, degrade power quality and energy output for long-spread networks considerably. Since a frequency drift which is earlier than usual, is subjected to the static threshold of UVR / OFR, the frequency perturbation had to be set higher to meet the sensitivity of the relays for all quality factor conditions. Impedance measuring techniques in this regard demonstrate a superior detection response, reduced NDZ, and less compromised power quality compared to classical active methods. These techniques may use fundamental frequency or sub/inter harmonic components as injection signals to the EPS. Despite their sophisticated methodology, these methods encounter various limitations, among which, the canceling effect during parallel operation of multiple inverters is one of the prominent. When multiple inverter-based DERs with the synchronous harmonic injection are connected to an EPS, they may contribute collectively a closed-loop current control of voltage source for a specific harmonic to the system. This may lead to transient instability of the system, flickering, and magnetic saturation issues for the electromagnetic components in an EPS. Another limitation of these techniques is their interference with the control and protection system (as many EPS protections are based on harmonic currents including earth faults).

For this reason, a sophisticated inverter control, is required to resolve the canceling effect problem. Few communication-based techniques including [30] propose a complex control scheme whose effectiveness is still questionable due to its ambiguous reliability concerns. However, micro-inverters-based techniques are getting quite popular these days for their modular approach and their effectiveness in regards to the canceling effect, without communication between parallel operating inverters. A comprehensive mathematical framework for sub/inter harmonic current injection and their limitations, especially in the case of parallel operation of DERs is discussed in [31]. The paper proposes an effective strategy to deal with the distortion effect of Pdc-MICs output and the canceling effect (compensating integer multiple of synchronous harmonic injections to the EPS) by means by introducing a time delay parameter in the control loop.

Another harmonic injection-inspired design and simulation technique for flyback inverters application is discussed in [32]. This technique presents a comprehensive framework for the parallel operation problem as discussed above. A deviation of 12-17% between the experimental and simulated results was observed during the analysis, however, an improved 4% THD was claimed for a 0.2 second window. In [33], an innovative open loop, low magnitude harmonic injection technique is presented for PV MICs with pseudo-dc-link. This technique, unlike the impedance estimation technique, uses a cross correlation-based estimation for grid operating conditions. The technique requires relatively less computational burden and is presents as an effective alternative over other active power techniques. It claimed to have THD for PCC voltages and inverter current of 7.5%and 4.2%, respectively which complies with the standard IEC 61727 [34]. Ahmed Mohamad *et al.* in [35] presented a nonlinear impedance estimation-based technique addressing the instability concerns of a grid-tied inverter using two active islanding methods. Experimental validation for the proposed scheme was also presented.

Hybrid methods are also getting popular in order to address the power quality concerns and canceling effect issues for active methods. [36] discusses a hybrid scheme based on the probability of islanding. This technique uses neuro-fuzzy controls with wavelet decomposition along with the active method. Not all quality factor conditions were considered in this technique however, a very low THD of 2.14% was claimed at the micro-grid end. In [37], a time-tested d-axis current injection technique is proposed which claims improved stability along with a fast response of 130 milliseconds during power mismatch conditions. This technique claims compatible operation for quality factor values ranging between 1.8 and 2.5. Another similar hybrid technique that utilizes THD plotting includes [38]. It uses the Gibbs phenomenon occurring at the interpolation of the sinusoidal function. Positive feedback is presented in this technique which monitors the real-time values of THD along with an effective offline validation scheme. This paper claims an accuracy of 69-89% on single and multi-inverter systems respectively with a THD of 1.32%. Other recently developed methods include [39] and [40] which uses comprehensive

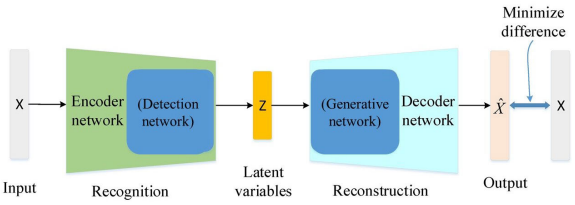

FIGURE 3. Auto-Encoder (AE) architecture.

characteristic analysis of voltage unbalances and THD for islanding detection.

III. AUTO-ENCODERS FOR ANOMALY DETECTION

Anomaly detection methods (ADMs) are usually classified as unsupervised or semi-supervised learning algorithms, which are trained over some anticipated/normal data and are tested to distinguish any data that deviates from the normal, which is classified as an anomaly. Some of the classical ADM includes gaussian mixture models (GMM) [41], bayesian models [42], K-nearest neighbour (KNN) [43], SVM [44] and other clustering algorithms.

Auto-Encoders (AE) belongs to the family of unsupervised ADM which is a higher dimensional reconstruction of principal component analysis (PCA) [45], [46]. Autoencoders are very effective in dimensionality reduction for complex non-linear functions using neural networks. Autoencoders are simpler neural networks but highly efficient generative models which consist of an encoder (a detection network) and a decoder (a generative network) which compresses the normal data and then recreates a series of data with the help of a low-resolution hidden neural network layer(s) to match the real data, as shown in Fig.3.

The encoder uses a cost function that tends to minimize itself over the epochs to generate a closely matched output to the input. The encoder function consists of three parameters: the Root mean squared error (RMSE), the L2 regularization index, and the sparsity regularization index, mathematically expressed as (7).

Using an encoder's cost function for any nonlinear signal application, there is always a significant risk of over-fitting the data. When a cost function is designed to fit exactly all the higher-order featured variables, it can no longer distinguish between the desired signal and the noise around it. In such a situation, the model is regarded as over-fit and it strictly tries to fits the input data which can lead to false detection/recognition. This over fitting problem in the cost functions can be regularized by an additional compensation term that either nullifies or attenuates the effects of unimportant higher-order featured variables by various means. This process of compensating the higher-order features, to avoid over-fitting or denoising of the data by dimensional reduction, is called regularization. Regularization includes an index as a fixed gain which is multiplied with a function which is explicitly dependent on the featured variable. The nature of this function can vary with the model or data application; however, the regularization index always remains a hyper-tuned constant.

In autoencoders, we have used two different regularizations, i.e. sparsity and L2 regularization. Auto-encoder's input matrix usually consists of sparse matrices which are higher dimensional input representations of the extracted features, this may introduce a computational limitation on the analysis along with the previously discussed over-fitting issue. L2 regularization penalizes by virtue of a squared function of the weights of the neural network, i.e. $w_{ij}{}^2$, where i and j represent the order of neurons in the input and hidden layer respectively. The derivative of the squared weight regularization function is a linear function $2w$ which can be interpreted as a percentage representation of the preceding values of the weights and for this reason, it can never be equal to zero. Sparsity regularization here, refers to Kullback-Leibler divergence. The purpose of this regularization is to minimize the difference between the desired activation value of a neuron and the average activation value of a neuron, to minimize the cost function. The main advantage of autoencoders is their capability to recognize nonlinear anomalies with a minimal computational cost by using dimensional reduction.

$$E = \frac{1}{N}\sum_{n=1}^{N}\sum_{k=1}^{K}(x_{kn} - \hat{x}_{kn})^2 + \lambda\ \Omega_w + \beta\ \Omega_s \tag{7}$$

where,

$$\Omega_w = \frac{1}{2}\sum_{l}^{L}\sum_{j}^{n}\sum_{i}^{k}(w_{ij}{}^{(l)})^2 \tag{8}$$

$$\Omega_s = \sum_{i=1}^{D^{(1)}} \rho\ log(\frac{\rho}{\hat{\rho}_1}) + (1-\rho)\ log(\frac{1-\rho}{1-\hat{\rho}_1}) \tag{9}$$

$$= \sum_{i=1}^{D^{(1)}} KL(\rho\ ||\ \hat{\rho}_1) \tag{10}$$

L = *numberofhiddenlayers*
n = *numberofobservations*
k = *numberoftrainingdata*
ρ = *desiredactivationvalueforneuroni*
$\hat{\rho}_1$ = *averageactivationvalueforneuroni*

IV. METHODOLOGY

This paper proposes a hierarchical layered strategy for islanding detection. Since the behavior of electrical power systems with distributed generation can be challenging to predict, a dialectic mode of validation is also proposed, which consists of online and offline validation schemes. The methodology is divided into three fundamental layers: a classical layer, an intelligent detection layer, and an online validation layer.

The classical layer is based on active frequency drift which is deployed in the inverter controls of the local DER. This layer, under islanding conditions, is used to create a frequency drift in the PCC voltage by injecting a very small perturbation

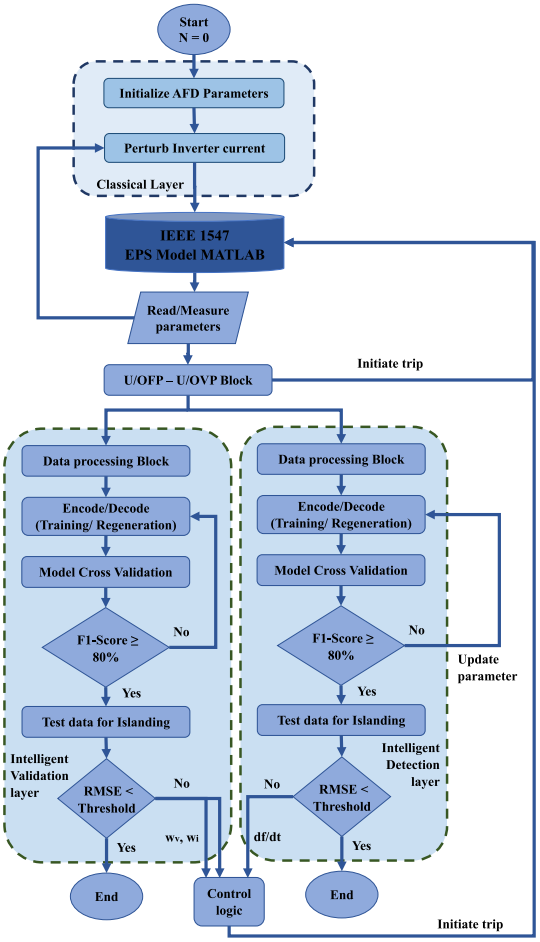

FIGURE 4. Process flow diagram for the methodology.

in the inverter current. This causes the frequency-dependent parameters to rise earlier than usual under islanding conditions and thus it can be detected effectively by the intelligent layer.

The intelligent detection layer is responsible for training and offline validation for the autoencoder on the rate of change of frequency parameter, discussed in section IV. The trip threshold for detection is selected based on offline validation statistics. This layer also regulates autoencoder's performance by ensuring its F1-score to be above 0.80.

The online validation layer works in parallel with the intelligent detection layer to validate the methodology in real-time. In this layer, another autoencoder is trained on the secondary parameters (phase angle pulse widths of PCC voltage and inverter current) and is used to detect islanding for various offline validation cases like the previous layer. Finally, a trip signal to DER control is then initialized using a logic design that ensures true-positive detection. The process flow diagram for the methodology is shown in Fig. 4.

A. THE CLASSICAL LAYER: ACTIVE FREQUENCY DRIFT (AFD)

In the classical layer, the frequency drift operation for the inverter current is achieved by initializing a chopping

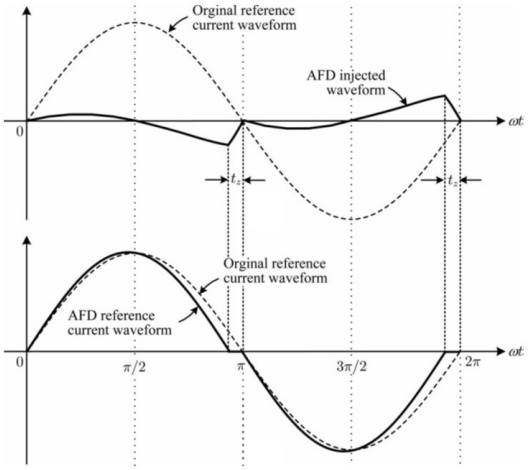

FIGURE 5. Frequency drift operation for AFD [47].

factor (cf). This chopping factor is proportional to the dead time (t_z) of the inverter current which is used as an active perturbation and is defined as (11). This dead time is usually so small that the corresponding value of differential frequency component (dF) has an insignificant impact on the power quality of the system. After the initialization of the design parameters for AFD, the inverter current function is redefined as (12) and is graphically expressed as Fig. 5.

$$cf = \frac{2t_z}{T_v} \tag{11}$$

$$i_{pcc}(t) = \begin{cases} I_{max}\ sin(2\pi f' t) & \text{if } 0 \le \omega' t \le \pi - t_z \\ 0 & \text{if } \pi - t_z \le \omega' t \le \pi \\ I_{max}\ sin(2\pi f' t) & \text{if } \pi \le \omega' t \le 2\pi - t_z \\ 0 & \text{if } 2\pi - t_z \le \omega' t \le 2\pi \end{cases} \tag{12}$$

where, $f' = f_{pcc} - df = f_{pcc}/(1 - cf)$, is the perturbed system frequency.

During islanding conditions, the frequency of the DER tends to drift earlier than usual. This frequency drift in inverter current induces a phase error between the inverter current and PCC voltage. This causes the voltage to drift further and further to catch the rising phase error thereby drifting frequency at PCC to a threshold where it can be detected as islanding.

The steady-state reactive power supplied under islanding is equal to the reactive power supplied by the DER and for this reason, the inverter angle under islanding conditions is equal to the load angle. This relationship between inverter and load angle is called phase criteria and is essential to determine the non-detection zone of the technique. A typical relationship of phase criteria in (C_{res} vs L) and (Q_f vs f_o) space are respectively given as:

$$arg\ (\frac{1}{R} + \frac{1}{j\,w\,L} + j\,w\,C)^{-1} = 0.5\,\pi\,cf \tag{13}$$

$$f_o{}^2 + \frac{tan\ \theta_{inv}(f)}{Q_f} f_o - f^2 = 0 \tag{14}$$

where, f_o is the resonant frequency of the load.

TABLE 1. Analyzed learning features.

Parameter	Description
df/dt	Rate of change of PCC frequency
dV/dt	Rate of change of PCC voltage
$d\theta_{AFD}/dt$	Rate of change of inverter angle
ω_{vph}	Phase-angle pulse width of PCC Voltage
ω_{Iph}	Phase-angle pulse width of DER Current
dV/dP	Rate of change of PCC voltage wrt to active power

B. THE INTELLIGENT DETECTION LAYER: UNSUPERVISED LEARNING

After the implementation of AFD under normal operating conditions, numerous features are listed in Table. 1, were critically analyzed for unsupervised detection using autoencoders. Finally, two of the best features were selected for detection and online validation criteria.

The rate of change of frequency was selected as a learning parameter for the detection layer due to its superior accuracy and F1-score. Initially, the data was retrieved from the EPS using a measuring block and then this data with unwanted starting transients was processed and split into training and offline validation cases in the data processing block. The data was then ready for encoding/decoding operation, followed by its training at the autoencoder. An autoencoder uses a feed-forward neural network with a backward propagation over the epochs to regenerate a signal which closely matches the normal/training data. This process is regulated by the encoder cost function until the training error is greatly minimized to a threshold root mean square error (RMSE) selected based on the validation cases.

Once the autoencoder is trained, the encoder is subjected to the offline validation cases. Under normal conditions, the real-time data matches the predicted data and as a result, the RMSE has a low value. But as soon as the islanding conditions are met, the actual data mismatch the predicted data and hence, the RMSE rises drastically until it reaches the set threshold, thereby detecting the islanding event. The offline validation cases consist of commonly occurring extreme events such as fault ride through, load addition and rejection, multi-inverter, and unbalanced system scenarios. In order to regulate the methodology, these cases are compelled to meet an F1-score of at least 0.80, as shown in Fig. 4.

C. THE ONLINE VALIDATION LAYER

This layer provides a real-time validation for the previous layer by performing a similar detection on the secondary parameters, i.e. phase-angle pulse width of the PCC voltage and the DER current. These features are also trained and validated using the autoencoders over the same validation cases and like the previous layer an F1-score of at least 0.80 is maintained for effective online validation. Since phase angle pulse width of PCC voltage, has a high false-positive ratio for multi-inverter models, a logic control was implemented which includes phase angle pulse width of DER current as a supplementary parameter that ensures true positive detection under multi-inverter cases.

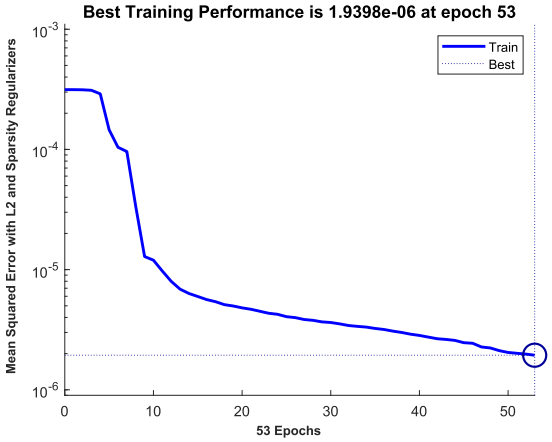

FIGURE 6. Performance curve for *df*/*dt* training.

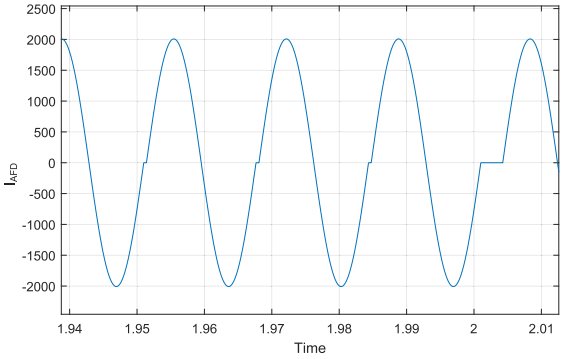

FIGURE 7. Simulated AFD waveform for df = 1 Hz.

V. MODELLING AND SIMULATION FOR ISLANDING DETECTION

Three test case models were designed to test islanding detection on Simulink MATLAB. These includes the IEEE 1547 standard model having a 120 kV bus on the grid side, a 575 V bus on the 2 MW Type 4 Wind farm side, and a 25 kV bus (at PCC) on the local load and circuit breaker side as shown in Fig. 1. The other two models includes IEEE 13 bus system with unbalanced load and IEEE 1547 model with Multiple DERs on the same bus. In the classical layer, AFD was implemented in the inverter control loop of the DER with a perturbation of df $=$ 1 Hz by mean of a hit-cross and discrete integrator function block. The islanding instant in the simulation was predefined to be 2 seconds as shown in the Fig. 7. All the necessary data of electrical parameters including df/dt, ω_{vph} and ω_{iph} was extracted to formulate a comprehensive data set for training the autoencoder.

A. TRAINING AUTOENCODER

The training in the intelligent detection layer was performed on 29,414 data points of time series data, for 500 maximum epoch, 30 hidden nodes, with L2 and sparsity regularization set for 1×10^6. The RMSE threshold for islanding detection

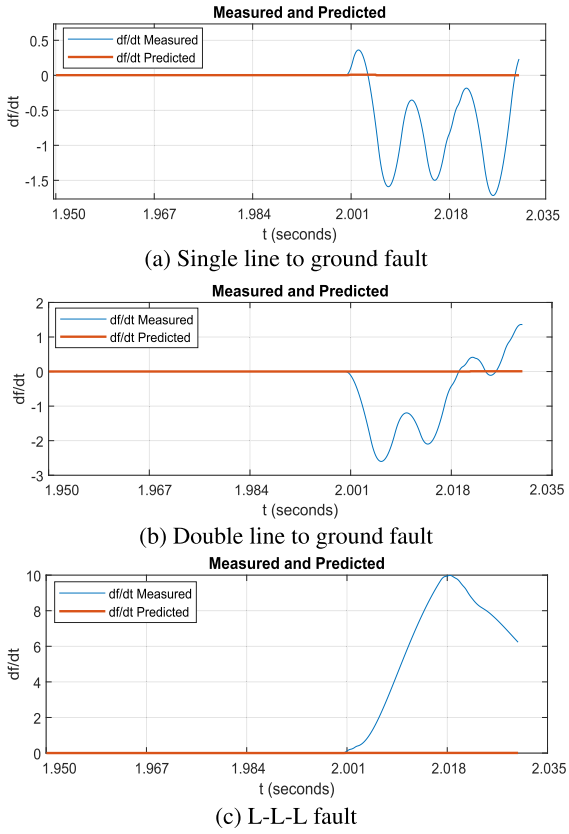

(a) Single line to ground fault

(b) Double line to ground fault

(c) L-L-L fault

FIGURE 8. Validation for fault cases.

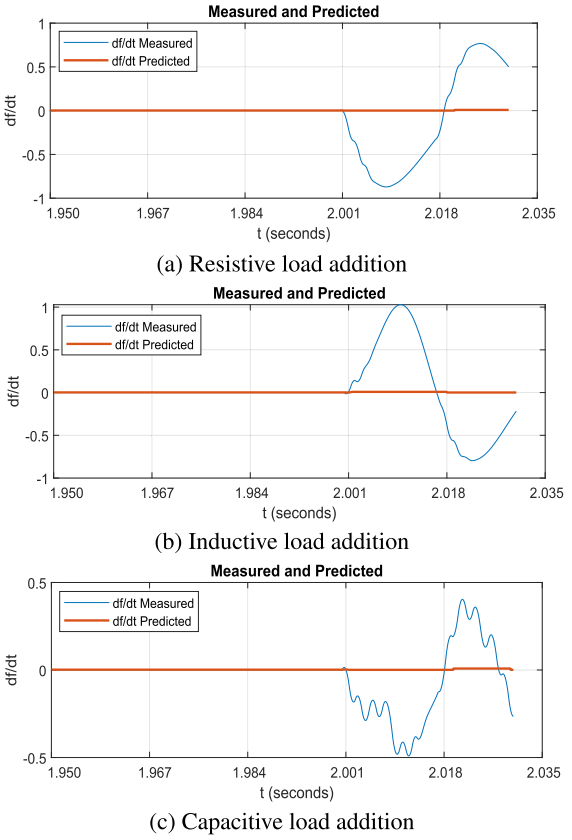

(a) Resistive load addition

(b) Inductive load addition

(c) Capacitive load addition

FIGURE 9. Validation for load addition cases.

was tested between 80 and 180, which was later fine-tuned at 110 for optimum F1-score, after analyzing the offline validations for the layer. The best training performance of the autoencoder for df/dt was achieved at RMSE $= 1.9398 \times 10^{-6}$ at the 53rd epoch, as shown in the performance curve Fig. 6.

B. OFFLINE VALIDATION

In order to test the validity and robustness of our proposed methodology, the anomaly detection experiment was validated offline for 14 different cases, such that each case was tested on 81 power mismatch scenarios, which makes a total of 1134 cases. Based on the nature of the events, these 14 cases were divided into the following four categories:

1) Typical cases: Normal operating conditions, early islanding conditions, and delayed islanding conditions.
2) Fault Ride through cases: Single line to ground (SLG) fault, double line to ground (DLG) fault, three-phase bolted (LLLG) fault.
3) Load addition and rejection cases: Resistive, capacitive and inductive.
4) Multi-inverter case (4 DER feeding the same bus) and Unbalanced system case

Among all of these 14 cases, only three cases represented actual islanding conditions, i.e. early islanding, delayed islanding under an unbalanced system whereas, all the rest of the cases were non-islanding events. Based on offline validation, an optimal threshold of 110 was chosen with an ideal F1-score of 0.991 on the test systems.

The RMSE function is proportional to the difference between the autoencoder's prediction of the parameter and actual measurement. An offline validation case for 10 percent active and 2.5 percent reactive power mismatch case are shown in Fig. 8, Fig. 9, Fig. 10, Fig. 11, and Fig. 12 for fault ride through cases, load addition and rejection cases, multi-inverter and unbalanced system cases, and typical cases, respectively. Islanding was successfully detected for the three true-positives, i.e. early (Fig. 11b) and delayed islanding (Fig. 11c), whereas all of the rest of the cases prevented false-positive detection.

C. ONLINE VALIDATION

For the online validation of the methodology it was observed that, during islanding conditions, the phase angle of PCC voltage has a very high disturbance which alters the pulse width instantly during islanding operation. This parameter has very high selectivity to false-positive cases, except for the case of the multi-inverter model. This is due to the fact that there may be power flows among the adjacent DER to the local loads, although the signature is smaller than local islanding but significant enough to initiate false-positive tripping.

In order to resolve this issue, another secondary parameter (phase angle pulse width of DER's current) was chosen

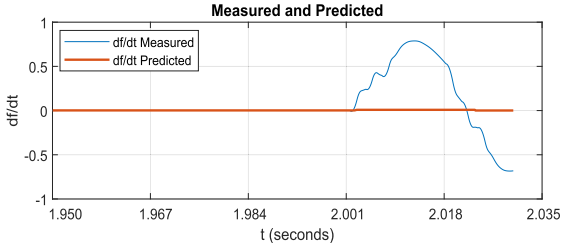

(a) Resistive load rejection

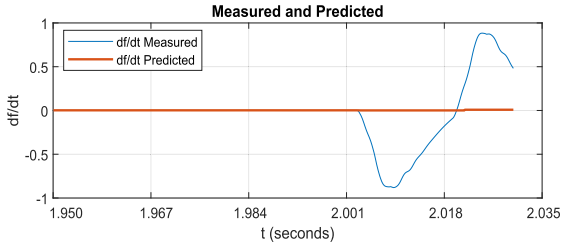

(b) Inductive load rejection

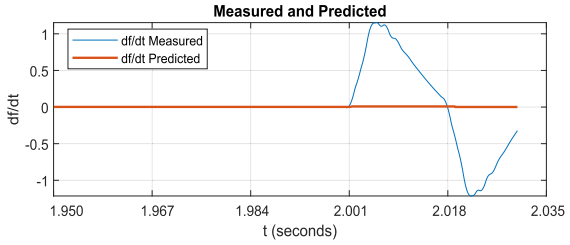

(c) Capacitive load rejection

FIGURE 10. Validation for load rejection cases.

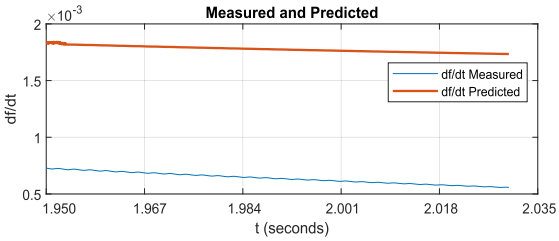

(a) Normal operating conditions

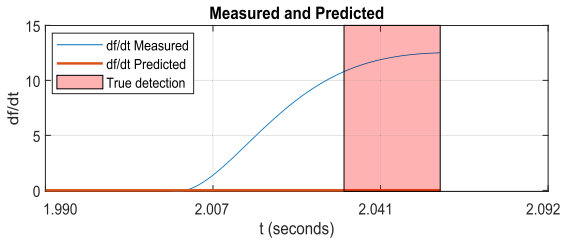

(b) Early islanding condition

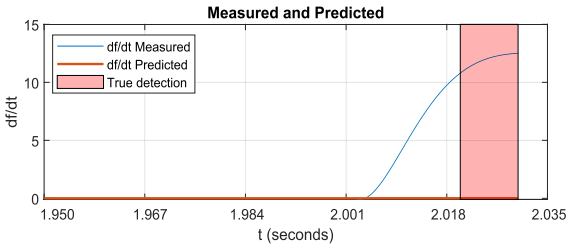

(c) Delayed islanding condition

FIGURE 11. Validation for typical cases.

TABLE 2. Truth table for the collective scheme.

ω_{vph}	ω_{Iph}	dV/dt	Action
0	0	0	Normal operating conditions.
0	0	1	Wait for validation.
0	1	0	Wait for primary pickup.
0	1	1	Wait for validation.
1	0	0	Wait for primary pickup.
1	0	1	Wait for validation.
1	1	0	Wait for primary pickup.
1	1	1	Initiate islanding alarm.

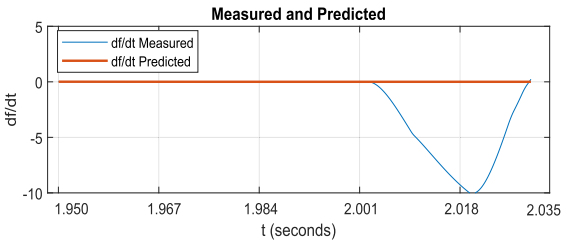

(a) Multi-inverter Case

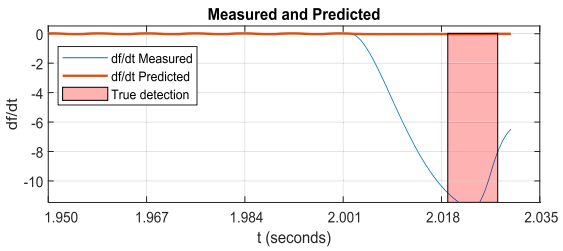

(b) Unbalanced system case

FIGURE 12. Validation for misc. cases.

in combination with the previous (phase angle pulse width of PCC voltage) for online validation. A logic control was finally designed in order to ensure a highly reliable and dependable scheme, as demonstrated in Table. 2. The online validation parameters, ω_{vph} and ω_{Iph} in the logic were AND together and this output was then again AND with the primary pickup parameter i.e. dV/dt. This online validation like the previous layer was also validated offline on the same, Fig. 20, Fig. 21 and Fig. 19 (see appendix).

For the load variation cases, a load variation of 10 percent of the active power mismatch and 2.5 percent of reactive power mismatch were simulated. All of those cases including the resistive, inductive, and capacitive load variations, could not produce RMSE above 60 and were able to distinguish between the load variation and islanding correctly. Even for the first batch of cases when the RMSE threshold was set to be 80, the highest value for RMSE was 11.1 for the case of capacitive load variation. The SLG and DLG fault, however, in all scenarios had RMSE less than the least threshold case, i.e. 60, and all fault ride through cases were distinguished from islanding at an RMSE threshold set for 110.

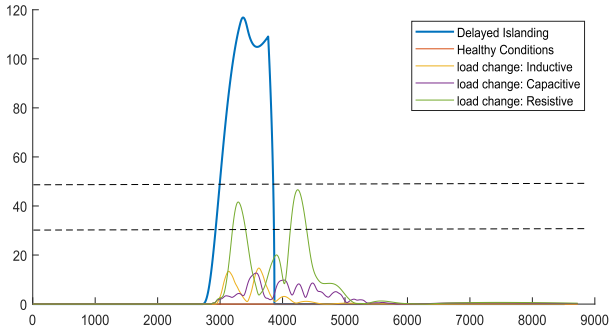

(a) RMSE for load variation cases

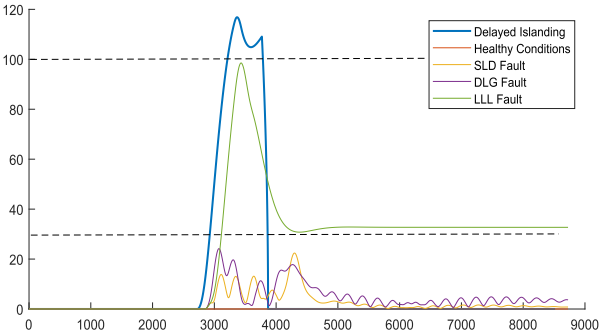

(b) RMSE for fault cases

FIGURE 13. Comparison of RMSE for validation cases.

Moreover, the comparison of RMSE threshold for all the validation cases for primary pickup are demonstrated in Fig. 13 which shows how the pickup values for RMSE were selected and selectivity of the protection was further reinforced by online validation characteristics. The RMSE threshold for both load variation cases an fault cases was selectively chosen such that no outliers lie within the selected threshold for accurate islanding detection..

D. PERFORMANCE INDICATORS

The performance of the proposed technique is advocated by means of three evaluation analysis, i.e. the analysis of the non-detection zone for all possible power mismatch conditions along with their respective detection times, the analysis of the statistical significance of the technique in terms of F1-score, and Harmonic analysis of the technique in terms of THD.

The non-detection zone analysis is done by simulating our proposed islanding detection scenario for every combination of active and reactive power mismatch by varying the loading conditions. The active power mismatch cases were simulated for values between $\pm 40\%$ with a step size of 10% (i.e. ranging from 1.2 MW to 2.8 MW) and the reactive power mismatch cases were simulated between $\pm 10\%$ with a step size of 2.5% (i.e. ranging from -400 MVAR to 400 MVAR) for all active mismatch cases. The detection time characteristics for power mismatch at 1.5 quality factor are shown in Fig.14a, which is compared to the performance of a traditional passive relaying with the proposed technique. Fig.14b demonstrates the variation in detection time concerning changing power mismatch

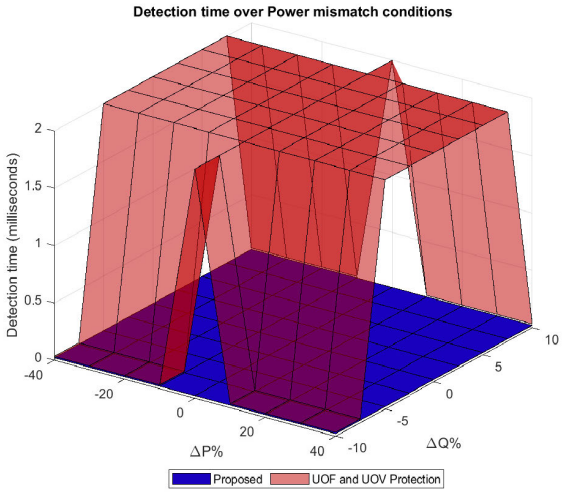

(a) Comparison of proposed technique with traditional passive relays.

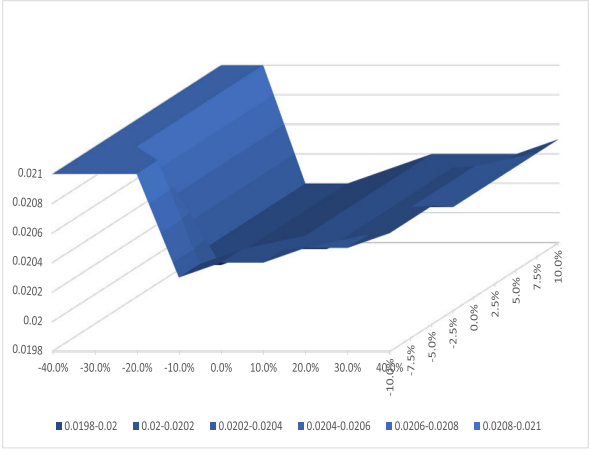

(b) Detection time characteristics for proposed technique.

FIGURE 14. Proposed technique under power mismatch.

conditions, with a mean of 20.4 milliseconds and a standard deviation of 0.00029. The comparison of detection accuracy with the other techniques in literature is presented in the discussion section.

The statistical analysis for the technique was done on the bases of its offline validations cases. The results of the analysis are summarized in the form of its confusion matrix for the 1134 cases in Fig. 15. It is evident from the matrix that the true positive rate and the true negative rate for the technique are quite high (100% and 99.5% respectively). The only miss-hit cases were the 4 three-phase bolted fault cases when the RMSE threshold was set below 110. This problem was resolved when RMSE was set to 110, augmented with the online validation feature that ensures the fault ride-through cases are not classified as islanding. With this inference, the islanding detection time was increased from 5.7 milliseconds to 20 milliseconds, but its robustness to distinguish between islanding and non-islanding events was greatly maximized.

The precision and f1-score response to all the 1134 offline validation cases is graphically expressed in 16a and 16b.

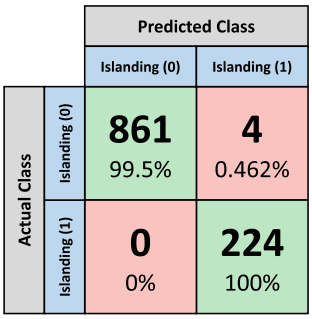

FIGURE 15. Confusion matrix - Statistical significance.

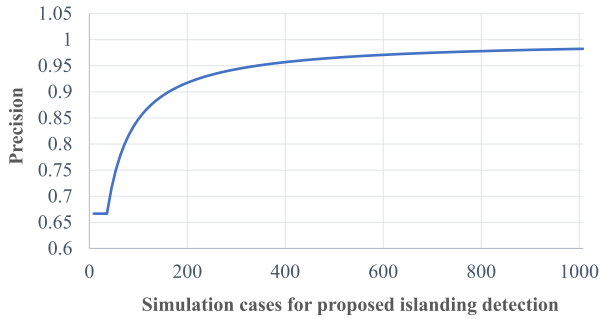

(a) Precision response

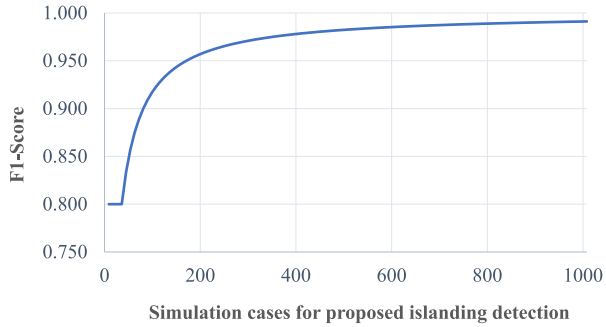

(b) F1-score response

FIGURE 16. F1-score and precision response.

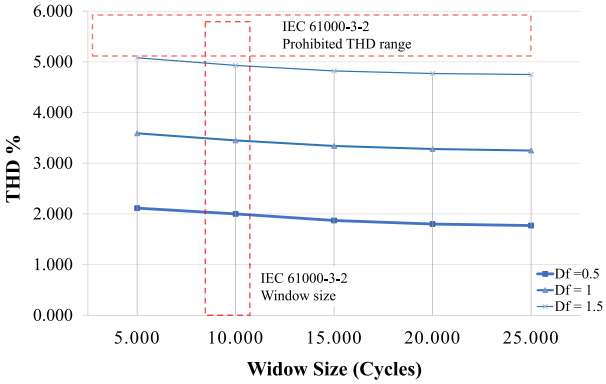

FIGURE 17. Effect of changing window size (cycles) on Total harmonic distortion in compliance with IEC 61000-3-2.

For the proposed technique, the recall, precision and f1-score were computed as 1.000, 0.982, and 0.991 respectively. The

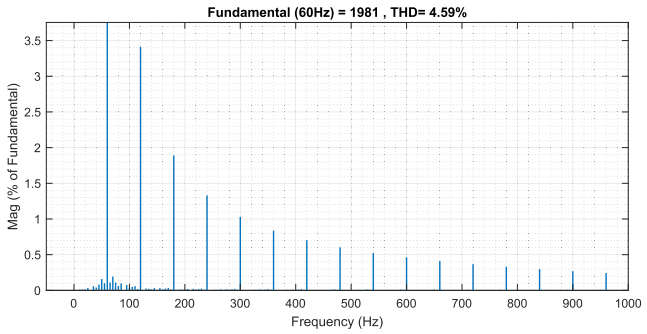

(a) Initialized at 1.5 second

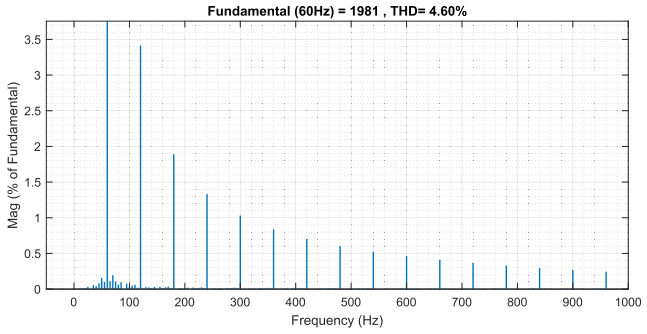

(b) Initialized at 2.5 second

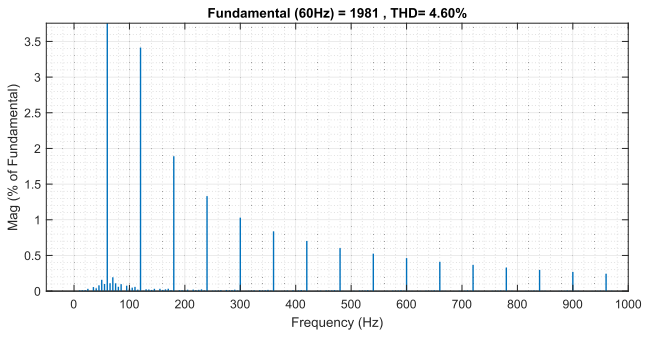

(c) Initialized at 3.5 second

FIGURE 18. FFT Plot for THD at different initialization.

dependability index (DI) and security index (SI) for the methodology was computed to be 99.8 and 99.5 percent respectively, which is a statistical proof for the effectiveness of the technique,

Active methods, in particular, encounters power quality issues due to harmonic injection in the inverter signals. IEC 61000-3-2 and IEC 61000-4-7 discusses the criteria for acceptable power quality standards for inverter-based anti-islanding techniques. According to the standard, the power quality measurements could be measured after 1.5s of filtering by means of a first-order filter, in a 200ms (10/12 cycle) window, with an overall allowable THD of $\pm 5\%$, with repeatability. The standard also discusses the benchmark for individual odd harmonics levels, such as for class A and B, the third harmonic should not exceed 2.3% and 3.45% respectively and the fifth harmonic should not exceed 1.14% and 1.71% respectively, and so on. [48] and [49] discuss anti-islanding techniques which demonstrate a detailed power quality analysis in terms of THD, voltage flickering, and grid penetration under weak grid conditions.

TABLE 3. Technical comparison of recently developed islanding detection techniques.

Technique	Type	Concept / Feature	DI and SI / Accuracy	Attributes	System type
Proposed scheme.	Hybrid intelligent	f, V and I phase angle	DI = 0.998 ; SI = 0.995	Zero NDZ, Very small detection time (20ms).	Standard radial, small scale Multi-inverter systems, unbalanced systems.
Two level Islanding detection method for DGs [56].	Hybrid intelligent	Wavelet entropy with AFD	-	Almost zero NDZ, Small detection time for both of the levels (> 0.3 s).	Single/two inverter system. No evidence for NDZ, power quality, DI and SI.
Hybrid scheme based on probability of islanding [36].	Hybrid intelligent	Neuro-fuzzy controls with wavelet decomposition along with the active method	-	Almost zero NDZ, Small detection time (> 2 cycles).	Single inverter systems, THD = 2.14%.
Hybrid d-axis current injection technique [37].	Hybrid	time-tested d-axis current disturbance injection	-	Almost zero NDZ, Small detection time (130 milli seconds).	Single inverter systems%.
Voltage Index based method [57].	Passive	f and V Index	-	Zero NDZ, Small detection time (< 0.3 s).	All DG configuration systems.
Deep learning based method [58].	Passive intelligent	Wavelet entropy with DL	Accuracy = 0.983	Almost zero NDZ, Small detection time (> 0.3 s)	Single inverter systems.
Extreme learning machine [50].	Passive intelligent	Hilbert–Huang transform	-	Almost zero NDZ, Small detection time (> 0.3 s).	All DG configuration systems.
Pattern recognition based approach [51].	Passive intelligent	8 wavelet coefficients for V and I	DI > 0.95 ; SI > 0.96	Difficult to design.	Conventional and inverter based DG.
Discrete wavelet transform [52].	Passive intelligent	3 wavelet coefficient for V	Accuracy >0.98	Small detection time (> 2 cycles)	Conventional DG.
Synchronous DG islanding protection using Intelligent relaying [53].	Passive intelligent	11 basic physical quantity (V)	DI > 0.98 ; SI> 0.45	Small detection time (> 2 cycles)	Conventional DG.
Sub/Inter-Harmonic Current Components based approach [31].	Active	Time delay parameter manipulation in the control loop	-	Almost zero NDZ, Small detection time (0.46 s)	Parallel operation of multiple inverters with high penetration in weak grid conditions, THD < 5%
Low magnitude harmonic injection technique for PV MICs with Pdc-link [33].	Active	Cross correlation-based estimation for grid operating conditions	-	Almost zero NDZ, Small detection time (0.4 s)	Parallel operation for multiple inverters with high penetration (> 30 %), THD < 4.2%
Harmonic Injection in an Interleaved Flyback Inverter [32].	Active	Second order harmonic injection using DFT	-	Small detection time (within 2 cycles)	Parallel operation for multiple inverters with high penetration (> 10 %), THD = 4.2%
Grid impedance estimation [55].	Active	Grid impedance injection	-	Zero NDZ, Small detection time (> 0.3 s).	Multiple inverter systems.

Power quality analysis for THD was carried out for the proposed strategy, in which the differential frequency between 0.5 to 1.5 was analyzed for cycles ranging from 5 to 25, as shown in 17. The maximum THD of a system for a window size of 12 cycle (200 milliseconds) was measured at different initialization, to confirm its validity (according to standard IEC 61000-3-2). Fig. 18a, 18b, and 18c demonstrates three different window selections for THD measurement at *df* set to 1.5. The average THD for the technique was measured to be 4.56%, which complies with the standard.

VI. DISCUSSION

In the light of performance indicators discussed in the previous section, the proposed strategy complies with all the standards with prominent results. The proposed methodology demonstrates a very high (dependability index) DI and (security index) SI with online and offline validation features in comparison to the techniques presented in the recent literature.

A technical comparison of the recently developed techniques for islanding detection is presented in Table. 3. Most of the techniques discussed here either have an intelligent design theme or have addressed power quality and gird penetration issues under weak grid conditions very effectively. In the table, passive methods based on wavelet entropy functions, parameter indices and pattern recognition [50]–[53], performs better on conventional systems however, most of the voltage and frequency based passive islanding

TABLE 4. Parameter limits by IEEE Standards.

Standard	IEEE Std. 929		IEEE Std. 1547	
Parameter	**Limit**	**Trip time**	**Limit**	**Trip time**
Voltage	V<60	6 cycles	V<60	0.16s
	60≤V≤106	120 cycles	60≤V≤106	2.0s
	106≤V≤132	Normal Operation	106≤V≤132	Normal Operation
	132≤V≤165	120 cycles	132≤V≤165	1.0s
	165≤V	2 cycles	144≤V	0.16
Frequency	59.3 - 60.5 Hz	Normal Operation	59.3 - 60.5 Hz	Normal Operation
	Other wise	6 cycles	Other wise	0.16
TDH %	<5%	Always	<5%	Always

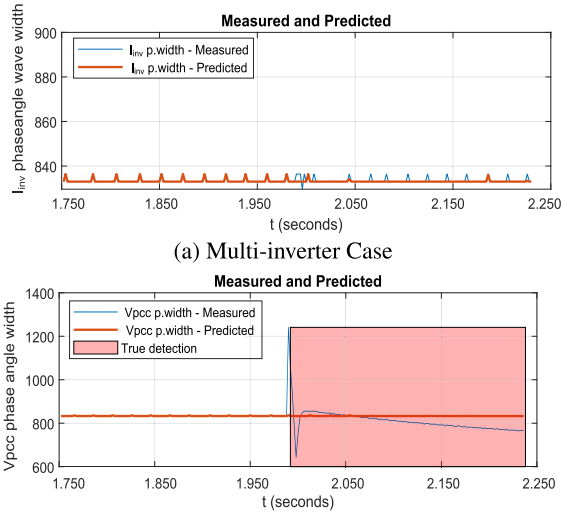

(a) Multi-inverter Case

(b) Unbalanced system case

FIGURE 19. Sec. validation: misc. cases.

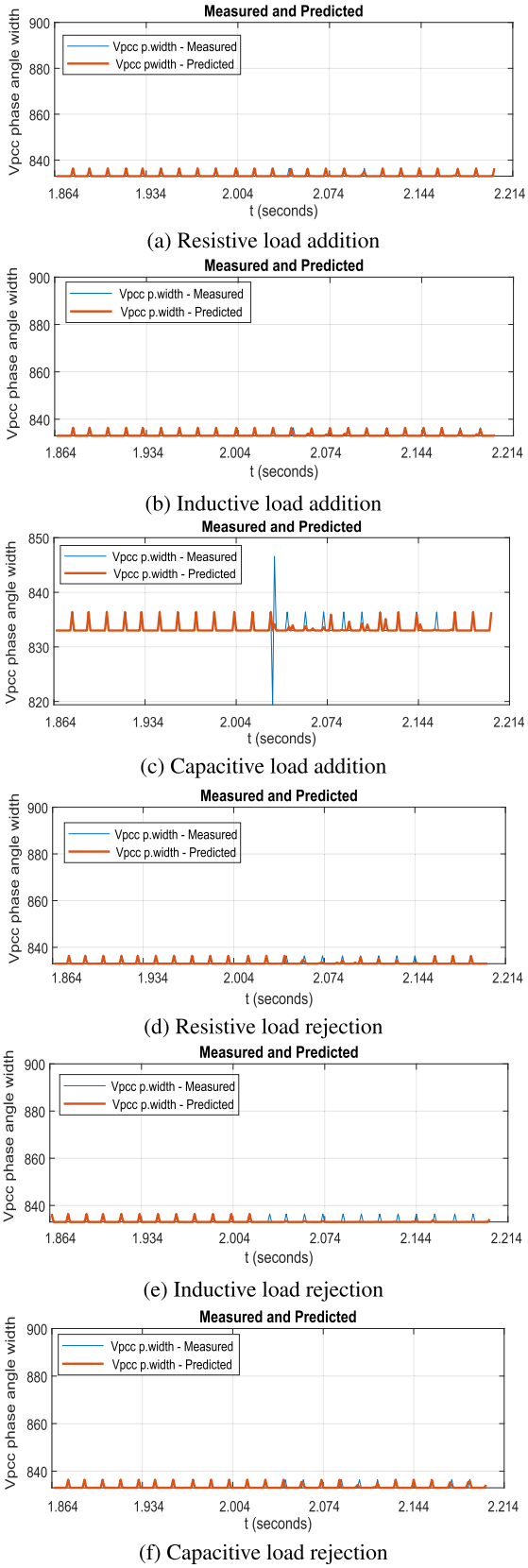

(a) Resistive load addition

(b) Inductive load addition

(c) Capacitive load addition

(d) Resistive load rejection

(e) Inductive load rejection

(f) Capacitive load rejection

FIGURE 20. Sec. validation: Load variation.

detection techniques are ineffective and less reliable for future power systems with high penetration of inverter-based DERs having high droop gains, i.e. grid supporting DERs as explained in [8]. However, deep learning-based passive techniques [9] in literature were found to have a very narrow range of validation scenarios of power mismatch conditions and false-positive conditions, along with a less dependable accuracy for the test case scenarios [54]. More than that, the recall for the techniques shows a greater room for improvements, as for various validation conditions, such as three-phase bolted faults, the neural network had to be trained using supervised learning which does not guarantee accuracy over the false-positive cases in anomaly detection application.

Active injection-based techniques especially impedance estimation and cross-correlation based on sub/inter harmonic injections [31]–[33], [55] are very effective in the case of parallel operation of inverters by managing synchronous harmonic injection through various techniques,

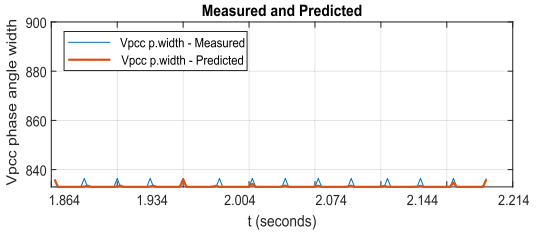

(a) Normal operating conditions

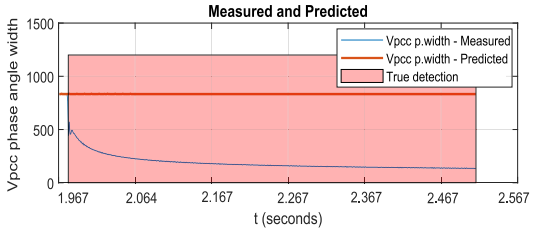

(b) Early islanding condition

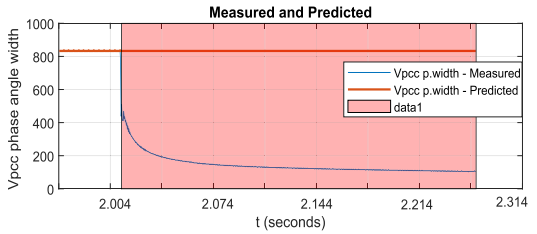

(c) Delayed islanding condition

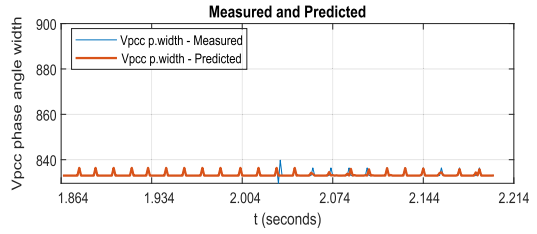

(d) Single line to ground fault

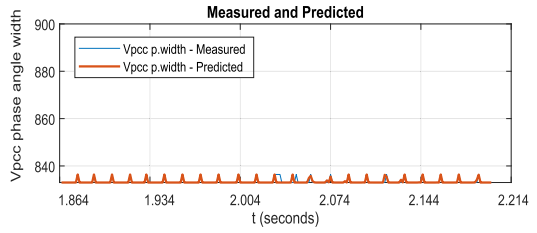

(e) Double line to ground fault

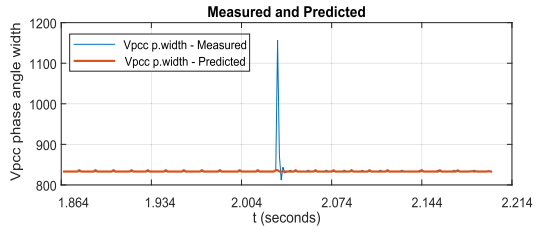

(f) L-L-L fault

FIGURE 21. Sec. validation: Typical and fault cases.

as discussed earlier. But due to their total reliance on estimation techniques for grid conditions, it usually requires complex, and computationally burdened controls for practical implementation. Also, it could be challenging to operate effectively under complex distributed generation systems due to their network dynamics which are evolving each day. On the other hand, the harmonic injection can frequently interact with control and protection schemes leading to a nuisance or unidentified trips, for example, in case of stator earth faults, they have a very strict pickup setting to third harmonics of the current, which can lead to repeated trips without any true stator earth faults. However, few recent techniques [33] have demonstrated very promising results for voltage flickering and grid penetration issues as shown in Table.3 and it could be made more reliable and dependable if these techniques could use an intelligent data-centric approach in the future.

Hybrid techniques, on the other hand, appear more promising as they can use two-level detection with minimum power quality compromise, lesser computationally burdened controls, unlike active methods. Traditional hybrid methods, including [37] are slower and less robust, however, the recent wavelet entropy of system parameters, which have intelligent algorithms, usually rely on single feature-based wavelet indices [9], [36], [56]. These techniques promise a high accuracy, along with a lacking of a definite validation scheme, which deteriorates its performance over false-positive islanding conditions. Unfortunately, even a very high accuracy in such cases does not guarantee reliability of the outcome, as it does not take account of multi-inverter system and unbalanced system especially in the case of three-phase bolted faults, which can be quite challenging to identify as non-islanding. More than that, Wavelet decomposition of a single variable to multiple indexes can be computationally rigorous and dimensionally less featured, as it does not account for other parameters that can contribute to islanding detection.

Unlike the recently published hybrid methods, our proposed methodology consists of a hierarchical layered approach. With its active frequency drifting feature, along with the intelligent generative model, it makes the technique computationally less burdened, due to its autoencoder-based, dimensional reduction scheme, with the least compromise on the system's power quality. Since the detection is done by the intelligent anomaly detection, which has a adaptive pickup (RMSE) unlike the traditional relays, the detection can be done with a very minimal harmonic injection, as low as a THD range of 1.77% - 4.56%. The proposed methodology due to its computational superiority is easily deployable using low processing programmable devices which would be totally self-reliant due to their data-centric approach.

The technique is primarily focused for grid following (current-source) inverters which are either operating as single inverter based DERs or as a small-scale parallel operating inverters on the adjacent buses such that they have a negligible harmonic canceling effect on the EPS. Since the proposed technique is based on intelligent islanding detection, it can work generically for the grid forming inverters (voltage-source) as well ideally, with a limitation of a complete inverter controls strategy for anti-islanding.

More than that, one of the prominent features of the proposed technique is its dialectical mode of validation. The offline validation ensures the selectivity of detection over extreme cases whereas, online validation uses three fundamental parameters for the detection, which ensures the probability of real-time true detection by means of control logic. These three parameters act as an online validation for each other, such that the performance of the technique cannot be bottle-necked by any one parameter, unlike in the past literature. Due to frequency drift operation in the classical layer, the selected three parameters are more prone to early islanding detection as compare to normal conditions with the least false positive ratio, which results in a quicker islanding detection (i.e. 20 milliseconds).

VII. CONCLUSION

This paper proposed a detailed methodology to design an intelligent islanding detection technique based on unsupervised learning, augmented by AFD. In the proposed technique, AFD was implemented in the inverter control of the DER, which exaggerated the voltage and frequency characteristics during islanding conditions. An autoencoder-based anomaly detection algorithm was deployed over the selected features, which were not only found effective for islanding detection using the intelligent regenerative strategy but also demonstrated an innovative approach to redefine programmable trip settings to training-based RMSE threshold settings. The technique also demonstrated an efficient strategy for online and offline validation. Different cases were simulated and tested for islanding in this validation technique, which includes fault ride-through cases, load variations cases, typical cases, multi-inverter/parallel operation, and unbalanced system cases. Furthermore, the effectiveness of the methodology was analyzed in terms of three performance indicators which include, NDZ for all possible power mismatch conditions, statistical significance, and power quality. The F1-score of 0.991, the dependability index of 0.998, the security index of 0.995, detection time of 20 milliseconds (IEEE 1547), and an allowable THD of 4.56% (IEC 61000-3-2) was measured with a zero non-detection zone. This advocates the technique to be a more reliable, dependable, and robust scheme for islanding detection for inverter-based distributed generation.

APPENDIX

See Table 4 and Figures 19–21.

ACKNOWLEDGMENT

The authors would like to thank entire team of Smart-grid laboratory, USPCAS-E, NUST, and Dr. Weng's laboratory for power systems, ASU for their technical support. They would also like to thank Faisal Mumtaz (PhD Scholar USPCASE, NUST), Shehzar Shehzad Sheikh (MS Scholar USPCASE, NUST), and Danyal Arif for their volunteer peer-review services.

REFERENCES

[1] IEA. (2020). *Renewables 2020, IEA, Paris*. [Online]. Available: https://www.iea.org/reports/renewables-2020

[2] *IEEE Recommended Practice for Utility Interface of Photovoltaic (PV) Systems*, IEEE Standard 929-2000, 2000.

[3] M. E. Ropp, "Design issues for grid-connected photovoltaic systems," Ph.D. dissertation, Dept. Elect. Eng., Georgia Inst. Technol., Atlanta, GA, USA, 1998.

[4] *IEEE Standard for Interconnection and Interoperability of Distributed Energy Resources With Associated Electric Power Systems Interfaces*, IEEE Standard 1547-2018 (Revision of IEEE Std 1547-2003), 2018, pp. 1–138.

[5] *IEEE Standard for Interconnecting Distributed Resources With Electric Power Systems*, IEEE Standard 1547-2003, 2003, pp. 1–28.

[6] R. A. Walling, "Application of direct transfer trip for prevention of DG islanding," in *Proc. IEEE Power Energy Soc. Gen. Meeting*, Jul. 2011, pp. 1–3.

[7] M. Ropp, P. Banschbach, C. Mouw, C. Mettler, and B. Enayati, "Application of pulse based power line carrier permissive (PLCP) in distribution system islanding detection," in *Proc. IEEE PES T&D Conf. Expo.*, Apr. 2014, pp. 1–6.

[8] U. Markovic, D. Chrysostomou, P. Aristidou, and G. Hug, "Impact of inverter-based generation on islanding detection schemes in distribution networks," *Electr. Power Syst. Res.*, vol. 190, Jan. 2021, Art. no. 106610.

[9] X. Kong, X. Xu, Z. Yan, S. Chen, H. Yang, and D. Han, "Deep learning hybrid method for islanding detection in distributed generation," *Appl. Energy*, vol. 210, pp. 776–785, 2018.

[10] W. Freitas, W. Xu, C. M. Affonso, and Z. Huang, "Comparative analysis between ROCOF and vector surge relays for distributed generation applications," *IEEE Trans. Power Del.*, vol. 20, no. 2, pp. 1315–1324, Apr. 2005.

[11] H. Samet, F. Hashemi, and T. Ghanbari, "Islanding detection method for inverter-based distributed generation with negligible non-detection zone using energy of rate of change of voltage phase angle," *IET Gener., Transmiss. Distrib.*, vol. 9, no. 15, pp. 2337–2350, Nov. 2015.

[12] R. Bugdal, A. Dysko, G. M. Burt, and J. R. McDonald, "Performance analysis of the ROCOF and vector shift methods using a dynamic protection modelling approach," in *Proc. 15th Int. Conf. Power Syst. Protection*, 2006, pp. 139–144.

[13] J. A. Laghari, H. Mokhlis, M. Karimi, A. H. A. Bakar, and H. Mohamad, "Computational intelligence based techniques for islanding detection of distributed generation in distribution network: A review," *Energy Convers. Manage.*, vol. 88, pp. 139–152, Dec. 2014.

[14] S. Alshareef, S. Talwar, and W. G. Morsi, "A new approach based on wavelet design and machine learning for islanding detection of distributed generation," *IEEE Trans. Smart Grid*, vol. 5, no. 4, pp. 1575–1583, Jul. 2014.

[15] T. S. Menezes, E. A. P. Gomes, D. V. Coury, and M. Oleskovicz, "A hybrid method for islanding stability detection of distributed generators using wavelet transform and artificial neural networks," in *Proc. Simposio Brasileiro de Sistemas Eletricos (SBSE)*, May 2018, pp. 1–6.

[16] H. Laaksonen, "Advanced islanding detection functionality for future electricity distribution networks," *IEEE Trans. Power Del.*, vol. 28, no. 4, pp. 2056–2064, Oct. 2013.

[17] M. A. Farhan and K. S. Swarup, "Mathematical morphology-based islanding detection for distributed generation," *IET Gener., Transmiss. Distrib.*, vol. 10, no. 2, pp. 518–525, 2016.

[18] H. Vahedi, G. B. Gharehpetian, and M. Karrari, "Application of duffing oscillators for passive islanding detection of inverter-based distributed generation units," *IEEE Trans. Power Del.*, vol. 27, no. 4, pp. 1973–1983, Oct. 2012.

[19] Q. Cui, K. El-Arroudi, and G. Joós, "Islanding detection of hybrid distributed generation under reduced non-detection zone," *IEEE Trans. Smart Grid*, vol. 9, no. 5, pp. 5027–5037, Sep. 2018.

[20] O. N. Faqhruldin, E. F. El-Saadany, and H. H. Zeineldin, "A universal islanding detection technique for distributed generation using pattern recognition," *IEEE Trans. Smart Grid*, vol. 5, no. 4, pp. 1985–1992, Jul. 2014.

[21] G. S. Rao and G. K. Rao, "An efficient islanding detection method in microgrids using hybrid SVM based decision tree," in *Proc. Int. Conf. Electr., Electron., Optim. Techn. (ICEEOT)*, Mar. 2016, pp. 601–607.

[22] L. A. C. Lopes and H. Sun, "Performance assessment of active frequency drifting islanding detection methods," *IEEE Trans. Energy Convers.*, vol. 21, no. 1, pp. 171–180, Mar. 2006.

[23] S. Akhlaghi, A. Akhlaghi, and A. A. Ghadimi, "Performance analysis of the Slip mode frequency shift islanding detection method under different inverter interface control strategies," *IEEE Trans. Energy Convers.*, vol. 21, pp. 1–7, 2016.
[24] H. H. Zeineldin and S. Conti, "Sandia frequency shift parameter selection for multi-inverter systems to eliminate non-detection zone," *IET Renew. Power Gener.*, vol. 5, no. 2, pp. 175–183, 2011.
[25] Q. Sun, J. M. Guerrero, T. Jing, J. C. Vasquez, and R. Yang, "An islanding detection method by using frequency positive feedback based on FLL for single-phase microgrid," *IEEE Trans. Smart Grid*, vol. 8, no. 4, pp. 1821–1830, Jul. 2017.
[26] Z. Xingchi, S. Anwen, and X. Jinbang, "Improved active frequency drift islanding detection method for grid-connected photovoltaic power generation system," in *Proc. 10th Int. Conf. Modeling, Identificat. Control (ICMIC)*, Jul. 2018, pp. 1–6.
[27] Y. Li, M. Hou, H. Feng, and X. Liu, "Composite islanding detection method based on the active frequency drift and voltage amplitude variation," in *Proc. IEEE PES Asia–Pacific Power Energy Eng. Conf. (APPEEC)*, Dec. 2014, pp. 1–6.
[28] D. Sivadas and K. Vasudevan, "An active islanding detection strategy with zero nondetection zone for operation in single and multiple inverter mode using GPS synchronized pattern," *IEEE Trans. Ind. Electron.*, vol. 67, no. 7, pp. 5554–5564, Jul. 2020.
[29] S. Murugesan and V. Murali, "Active unintentional islanding detection method for multiple-PMSG-based DGs," *IEEE Trans. Ind. Appl.*, vol. 56, no. 5, pp. 4700–4708, Sep. 2020.
[30] F. Briz, D. Díaz-Reigosa, C. Blanco, and J. M. Guerrero, "Coordinated operation of parallel-connected inverters for active islanding detection using high-frequency signal injection," *IEEE Trans. Ind. Appl.*, vol. 50, no. 5, pp. 3476–3484, Sep. 2014.
[31] D. Voglitsis, F. Valsamas, N. Rigogiannis, and N. Papanikolaou, "On the injection of sub/inter-harmonic current components for active anti-islanding purposes," *Energies*, vol. 11, no. 9, p. 2183, Aug. 2018.
[32] D. Voglitsis, N. Papanikolaou, and A. C. Kyritsis, "Incorporation of harmonic injection in an interleaved flyback inverter for the implementation of an active anti-islanding technique," *IEEE Trans. Power Electron.*, vol. 32, no. 11, pp. 8526–8543, Nov. 2017.
[33] D. Voglitsis, N. P. Papanikolaou, and A. C. Kyritsis, "Active cross-correlation anti-islanding scheme for PV module-integrated converters in the prospect of high penetration levels and weak grid conditions," *IEEE Trans. Power Electron.*, vol. 34, no. 3, pp. 2258–2274, Mar. 2019.
[34] *Systems. Characteristics of the Utility Interface*, IEC Standard, I.E.C. Photovoltaic, 2004, vol. 61, p. 727.
[35] A. M. I. Mohamad and Y. A.-R.-I. Mohamed, "Impedance-based analysis and stabilization of active DC distribution systems with positive feedback islanding detection schemes," *IEEE Trans. Power Electron.*, vol. 33, no. 11, pp. 9902–9922, Nov. 2018.
[36] S. D. Kermany, M. Joorabian, S. Deilami, and M. A. S. Masoum, "Hybrid islanding detection in microgrid with multiple connection points to smart grids using fuzzy-neural network," *IEEE Trans. Power Syst.*, vol. 32, no. 4, pp. 2640–2651, Jul. 2017.
[37] S. Murugesan, V. Murali, and S. A. Daniel, "Hybrid analyzing technique for active islanding detection based on d-axis current injection," *IEEE Syst. J.*, vol. 12, no. 4, pp. 3608–3617, Dec. 2018.
[38] D. Mlakić, H. R. Baghaee, and S. Nikolovski, "Gibbs phenomenon-based hybrid islanding detection strategy for VSC-based microgrids using frequency shift, THD_U, and RMS_U," *IEEE Trans. Smart Grid*, vol. 10, no. 5, pp. 5479–5491, Nov. 2018.
[39] X. Chen, Y. Li, and P. Crossley, "A novel hybrid islanding detection method for grid-connected microgrids with multiple inverter-based distributed generators based on adaptive reactive power disturbance and passive criteria," *IEEE Trans. Power Electron.*, vol. 34, no. 9, pp. 9342–9356, Sep. 2019.
[40] G. Wang, F. Gao, J. Liu, Q. Li, and Y. Zhao, "Design consideration and performance analysis of a hybrid islanding detection method combining voltage unbalance/total harmonic distortion and bilateral reactive power variation," *CPSS Trans. Power Electron. Appl.*, vol. 5, no. 1, pp. 86–100, Mar. 2020.
[41] N. Moustafa, G. Creech, and J. Slay, "Anomaly detection system using beta mixture models and outlier detection," in *Progress in Computing, Analytics and Networking*. Singapore: Springer, 2018, pp. 125–135.
[42] S. Aljawarneh, M. Aldwairi, and M. B. Yassein, "Anomaly-based intrusion detection system through feature selection analysis and building hybrid efficient model," *J. Comput. Sci.*, vol. 25, pp. 152–160, Mar. 2018.
[43] G. Serpen and E. Aghaei, "Host-based misuse intrusion detection using PCA feature extraction and kNN classification algorithms," *Intell. Data Anal.*, vol. 22, no. 5, pp. 1101–1114, Sep. 2018.
[44] Y. Tian, M. Mirzabagheri, S. M. H. Bamakan, H. Wang, and Q. Qu, "Ramp loss one-class support vector machine; a robust and effective approach to anomaly detection problems," *Neurocomputing*, vol. 310, pp. 223–235, Oct. 2018.
[45] D. J. Bartholomew, "Principal components analysis," in *International Encyclopedia of Education*, P. Peterson, E. Baker, and B. McGaw, Eds., 3rd ed. Amsterdam, The Netherlands: Elsevier, 2010, pp. 374–377. [Online]. Available: https://www.sciencedirect.com/science/article/pii/B9780080448947013580, doi: 10.1016/B978-0-08-044894-7.01358-0.
[46] I. T. Jolliffe and J. Cadima, "Principal component analysis: A review and recent developments," *Phil. Trans. Roy. Soc. A, Math., Phys. Eng. Sci.*, vol. 374, no. 2065, Apr. 2016, Art. no. 20150202.
[47] A. Yafaoui, B. Wu, and S. Kouro, "Improved active frequency drift anti-islanding detection method for grid connected photovoltaic systems," *IEEE Trans. Power Electron.*, vol. 27, no. 5, pp. 2367–2375, May 2012.
[48] D. Voglitsis, F. Valsamas, N. Rigogiannis, and N. P. Papanikolaou, "On harmonic injection anti-islanding techniques under the operation of multiple DER-inverters," *IEEE Trans. Energy Convers.*, vol. 34, no. 1, pp. 455–467, Mar. 2019.
[49] F. Valsamas, D. Voglitsis, N. Rigogiannis, N. Papanikolaou, and A. Kyritsis, "Comparative study of active anti-islanding schemes compatible with MICs in the prospect of high penetration levels and weak grid conditions," *IET Gener., Transmiss. Distrib.*, vol. 12, no. 20, pp. 4589–4596, Nov. 2018.
[50] M. Mishra, M. Sahani, and P. K. Rout, "An islanding detection algorithm for distributed generation based on Hilbert–Huang transform and extreme learning machine," *Sustain. Energy, Grids Netw.*, vol. 9, pp. 13–26, Mar. 2017.
[51] N. W. A. Lidula and A. D. Rajapakse, "A pattern recognition approach for detecting power islands using transient signals—Part I: Design and implementation," *IEEE Trans. Power Del.*, vol. 25, no. 4, pp. 3070–3077, Oct. 2010.
[52] M. Heidari, G. Seifossadat, and M. Razaz, "Application of decision tree and discrete wavelet transform for an optimized intelligent-based islanding detection method in distributed systems with distributed generations," *Renew. Sustain. Energy Rev.*, vol. 27, pp. 525–532, Nov. 2013.
[53] H. G. Far, A. J. Rodolakis, and G. Joos, "Synchronous distributed generation islanding protection using intelligent relays," *IEEE Trans. Smart Grid*, vol. 3, no. 4, pp. 1695–1703, Dec. 2012.
[54] S. Vyas, R. Kumar, and R. Kavasseri, "Unsupervised learning in islanding studies: Applicability study for predictive detection in high solar PV penetration distribution feeders," in *Proc. IEEE Uttar Pradesh Sect. Int. Conf. Electr., Comput. Electron. Eng. (UPCON)*, 2016, pp. 361–366.
[55] W. Ghzaiel, M. J.-B. Ghorbal, I. Slama-Belkhodja, and J. M. Guerrero, "Grid impedance estimation based hybrid islanding detection method for AC microgrids," *Math. Comput. Simul.*, vol. 131, pp. 142–156, Jan. 2017.
[56] S. Shrivastava, S. Jain, R. K. Nema, and V. Chaurasia, "Two level islanding detection method for distributed generators in distribution networks," *Int. J. Electr. Power Energy Syst.*, vol. 87, pp. 222–231, May 2017.
[57] A. G. Abd-Elkader, S. M. Saleh, and M. B. M. Eiteba, "A passive islanding detection strategy for multi-distributed generations," *Int. J. Electr. Power Energy Syst.*, vol. 99, pp. 146–155, Jul. 2018.

ADEEL ARIF (Member, IEEE) received the B.E. degree in electrical and computer engineering from the NED University of Engineering and Technology, Pakistan, in 2015. He is currently pursuing the M.Sc. degree in electrical power engineering with the U.S.-Pakistan Center for Advanced Studies in Energy (USPCAS-E), NUST. From 2015 to 2017, he worked as a Design and Execution Specialist in the domain of electrical protection and generation systems with the Schneider-Electric and FFBL 118 MW Coal Power Project. He is currently working as a Visiting Faculty Member at the NED University of Engineering and Technology. His current research interests include the application of statistical machine learning, deep learning, and reinforcement learning for explainable AI in optimization, control, and protection of distributed generation. He was awarded the USAID fully funded scholarship for his M.Sc. degree and a research exchange opportunity at the Machine Learning Laboratory for Power System, Arizona State University, in 2019.

KASHIF IMRAN received the B.Sc. and M.Sc. degrees in electrical engineering from the University of Engineering and Technology (UET), Lahore, in 2006 and 2008, respectively, and the Ph.D. degree in electrical engineering from the University of Strathclyde, in 2015, through the Commonwealth Scholarship. He has worked with the Transmission and Distribution Division, Siemens, and the Power Distribution Design Section, NESPAK, from 2006 to 2007. He has worked as a Faculty Member at the University of Engineering and Technology (UET) and COMSATS University Lahore. He has been the inaugural Head of the Department of Electrical Power Engineering, U.S.-Pakistan Center for Advanced Studies in Energy, National University of Sciences and Technology, Islamabad, since 2018.

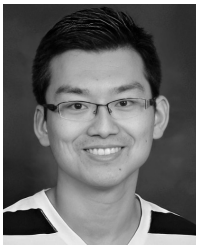

QIUSHI CUI (Member, IEEE) received the M.Sc. degree in electric engineering from the Illinois Institute of Technology and the Ph.D. degree in electrical engineering from McGill University. He was a Research Engineer with OPAL-RT Technologies, Inc., from 2015 to 2017. He is currently a Postdoctoral Scholar with the Ira A. Fulton Schools of Engineering, Arizona State University. His research interests include machine learning and big data applications in power systems, power system protection, smart cities, micro-grid, EV integration, renewable energies, and real-time simulation in power engineering. He was a recipient of the Best Paper Award at the 13th IET International Conference on Developments in Power System Protection, Edinburgh, U.K., in 2016, and the Chunhui Cup Innovation and Entrepreneurship Competition for Overseas Chinese Scholars in Energy Sector, in 2018. He received the Postdoctoral Research Scholarship from Le Fonds de recherche du Québec—Nature et technologies and held a Canada MITACS Accelerate Research Program Fellowship.

YANG WENG (Senior Member, IEEE) received the B.E. degree in electrical engineering from the Huazhong University of Science and Technology, Wuhan, China, the first M.Sc. degree in statistics from the University of Illinois at Chicago, Chicago, IL, USA, the second M.Sc. degree in machine learning of computer science, and the M.E. and Ph.D. degrees in electrical and computer engineering from Carnegie Mellon University (CMU), Pittsburgh, PA, USA. He joined Stanford University, Stanford, CA, USA, as a TomKat Fellow of sustainable energy. He is currently an Assistant Professor of electrical, computer, and energy engineering with Arizona State University, Tempe, AZ, USA. His research interests include power systems, machine learning, and renewable integration. He was a recipient of the CMU Deans Graduate Fellowship, in 2010; the Best Paper Award at the International Conference on Smart Grid Communication (SGC), in 2012; the First Ranking Paper of SGC, in 2013; the Best Papers at the Power and Energy Society General Meeting, in 2014; the ABB Fellowship, in 2014; and the Golden Best Paper Award at the International Conference on Probabilistic Methods Applied to Power Systems, in 2016.